Electronic Supplementary Information

H_2O_2-Triggered Shape Transformation of Silver Nanospheres to Nanoprisms with Controllable Longitudinal LSPR Wavelengths

Tewarak Parnklang, Chutiparn Lertvachirapaiboon, Prompong Pienpinijtham,
Kanet Wongravee, Chuchaat Thammacharoen, Sanong Ekgasit[*]

Sensor Research Unit,
Department of Chemistry, Faculty of Science, Chulalongkorn University
254 Phayathai Road, Patumwan, Bangkok 10330, THAILAND

[*] To whom correspondence should be addressed. E-mail: sanong.e@chula.ac.th
Telephone and Fax: (662) 218-7585

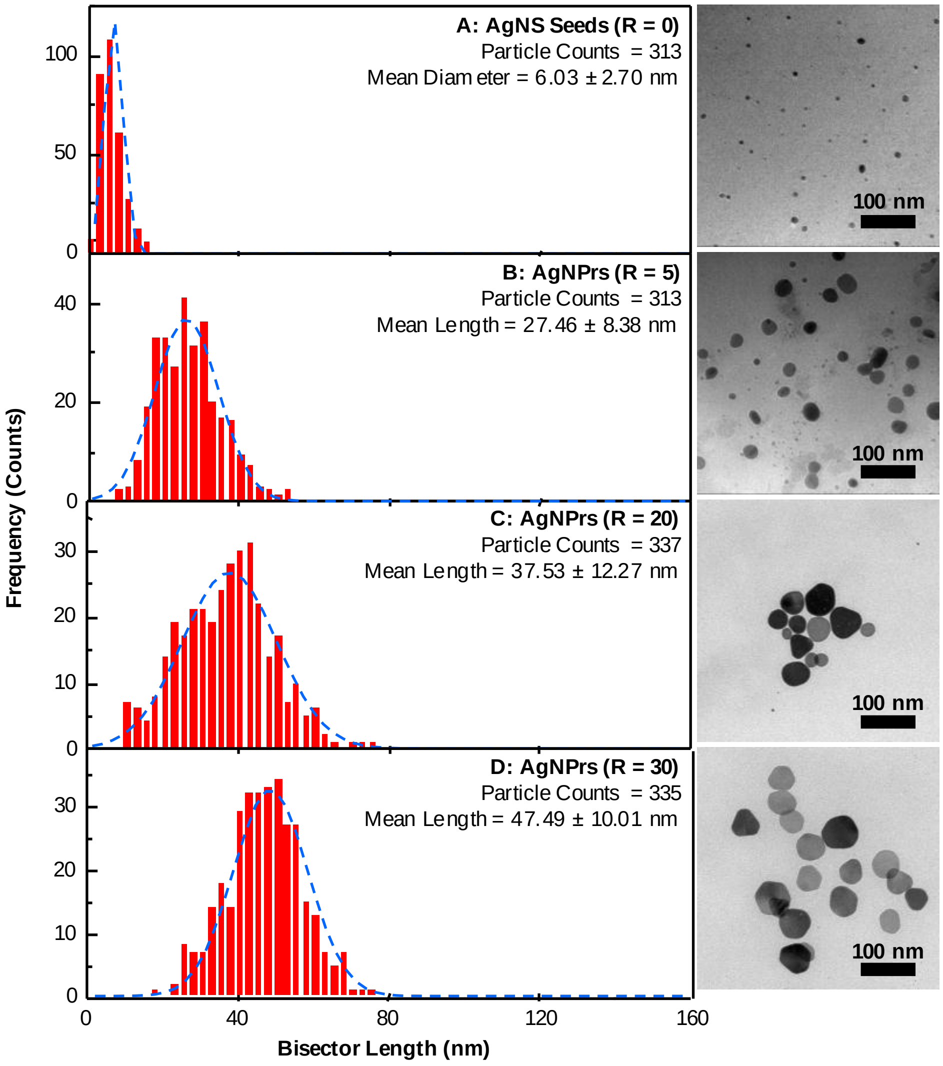

Fig. S1 Histograms show particle size distribution of the original silver nanospheres (AgNSs) (A) and the corresponding silver nanoprisms (AgNPrs) synthesized by the H_2O_2-triggered shape transformation with the mole ratio of H_2O_2:AgNSs (R) of 10 (B), 20 (C), and 30 (D). Each histogram was calculated from at least 300 particles in non-overlapping TEM images with sufficiently clear and adequate magnifications. Examples of the employed TEM images are shown. The particles show normal size distribution as indicated by the fitted Gaussian curves (dotted lines).

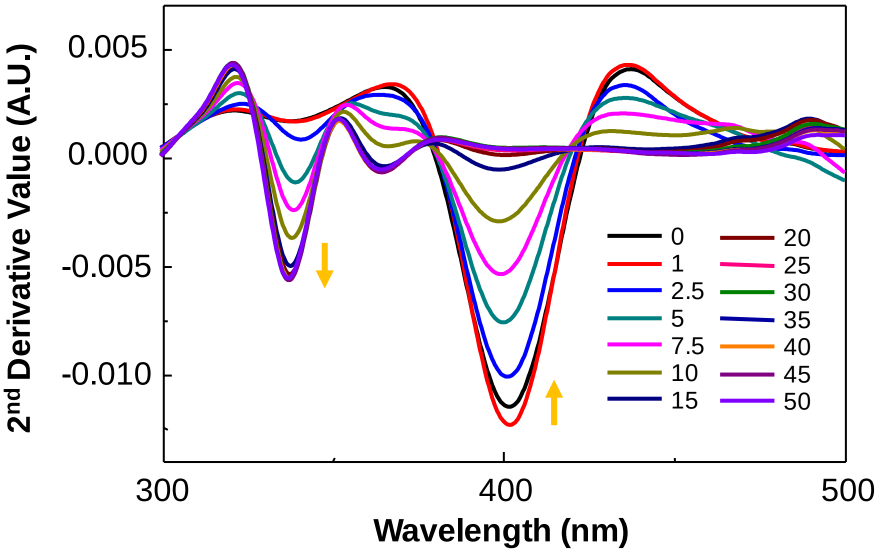

Fig. S2 2nd Derivative spectra of the plasmon extinction spectra shown in Fig. 1 (main text). The numbers indicate the molar ratio of H_2O_2:AgNSs (R) employed for the shape transformation process. The dipole plasmon resonance (DPR) of AgNSs at ~400 nm decrease while the out-of-plane quadrupole plasmon resonance (QPQPR) near ~340 nm increase as the mole ratio R increase.

Table S1 Peak positions of dipole plasmon resonance (DPR) of AgNSs, in-plane dipole plasmon resonance (IPDPR) and out-of-plane quadrupole plasmon resonance (OPQPR) of AgNPrs of the plasmon resonance spectra shown in Fig. 1 (main text). R indicates the molar ratio of H_2O_2:AgNSs employed for the shape transformation.

R	OPQPR of AgNPrs	IPDPR of AgNPrs	DPR of AgNSs
0	Not Observed	Not Observed	401.85
1	Not Observed	Not Observed	401.85
2.5	340.88	Not Observed	401.14
5	339.07	511.61	400.06
7.5	338.70	523.06	339.35
10	337.98	541.19	398.99
15	337.61	559.72	398.99
20	337.61	570.14	Not Observed
25	337.25	573.55	Not Observed
30	337.25	574.57	Not Observed
35	337.25	581.11	Not Observed
40	337.25	582.72	Not Observed
45	337.25	584.08	Not Observed
50	337.07	594.12	Not Observed

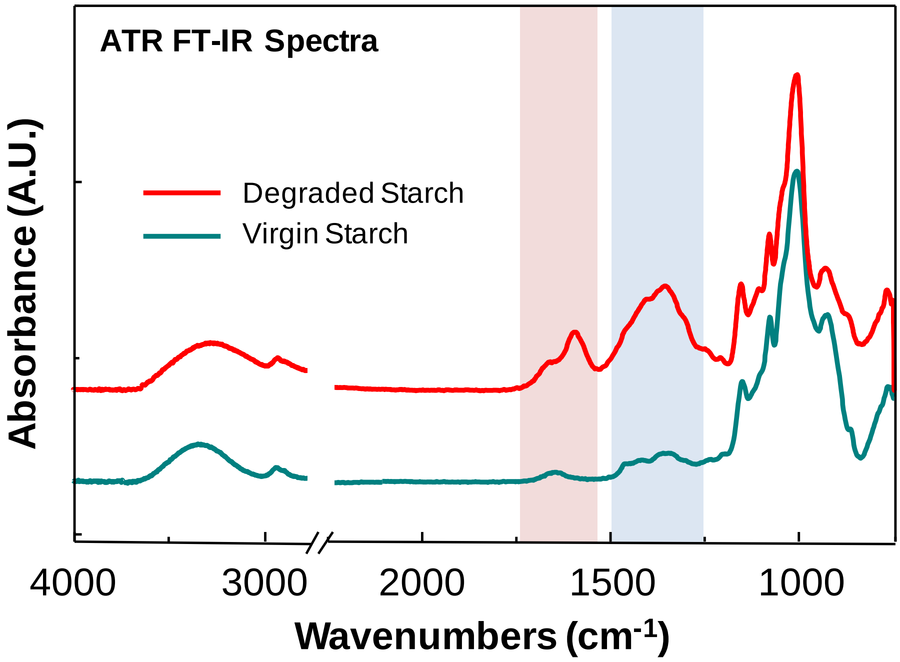

Fig. S3 Comparison of ATR FT-IR spectra of virgin starch and degraded starch. The partially degraded starch was prepared by subjecting the virgin starch to a consecutive acidic/alkaline treatment.

To make soluble starch an efficient reducing agent, the starch must undergo (i) acidic hydrolysis and (ii) alkaline treatment in order to induce a formation of degradation intermediates containing alpha-hydroxy ketone or aldehyde functionality. The operation must be performed under a hot alkaline solution (pH 12-14, 80-100 °C: P. Pienpinijtham *et al.*, *Macromol. Res.*, 2012, **20**, 1281–1288. and D. Tongsakul *et al.*, *Carbohydr. Res.*, 2012, **357**, 90–97.). The sign of starch degradation is evident via the distinct development of the absorption centered at 1591 and 1354 cm^{-1} (as indicated by the pink and blue bands, respectively) assigned to asymmetric and symmetric vibration of the carboxylate (-COO$^-$) group. Insignificant changes of the absorptions at 1200-900 cm^{-1} of the glycosidic linkage (bridge β C^1–O–C^4 stretching) and the absorption at 939 cm^{-1} of the skeleton vibration of α-1,4 glycosidic linkage (C–O–C) suggest that the degradation is partial. The absorption at 1634 cm^{-1} is assigned to the water absorption in the amorphous starch (R. Kizil, J. Irudayaraj, and K. Seetharaman, *J. Agric. Food Chem.*, 2002, 50, 3912).

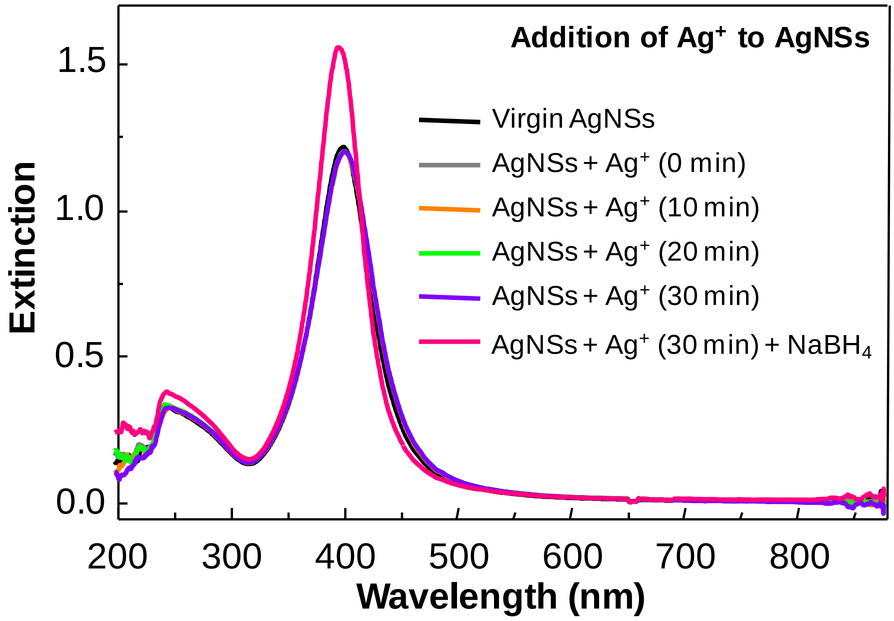

Fig. S4 Plasmon extinction spectra of 3.52 mM AgNSs incubated with 0.46 mM Ag^+. The colloid incubated for 30 min shows no sign of change. However, after an addition of a trace amount of $NaBH_4$, a sudden increment of the DPR at ~400 nm of AgNSs is observed.

To investigate the reducing capability of starch, we did add $AgNO_3$ into the colloid of AgNSs. No change was observed even after 30 min incubation. This observation indicates that the as-synthesized starch-stabilized AgNSs colloid with a mild alkaline condition (pH 8-9) is absent of residual $NaBH_4$ reducing agent while starch does not reduce the added Ag^+. However, when $NaBH_4$ was added, the increased DPR extinction at ~400 nm indicates a formation of additional AgNSs derived from the added $AgNO_3$. The observed phenomena confirm that starch is not a reducing species in the shape transformation process. It functions as the sole stabilizer.

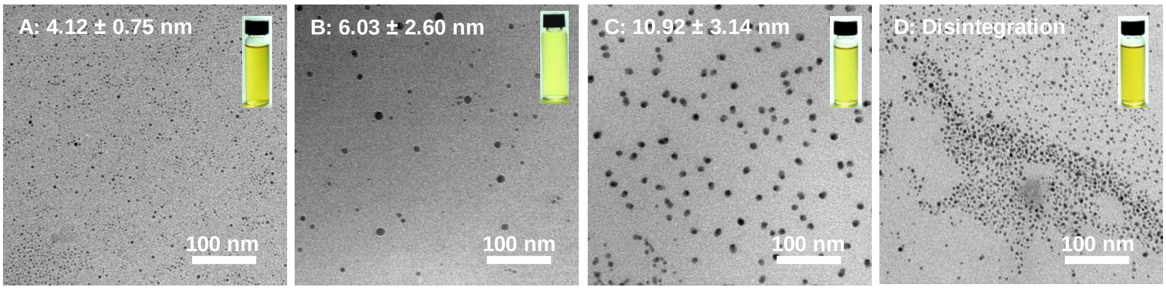

Fig. S5 TEM micrographs of AgNSs synthesized by reducing $AgNO_3$ solution with aqueous $NaBH_4$ with the presence of 2% (w/v) soluble starch with [$AgNO_3$] of 0.14 mM (A) and 3.71 mM (B). Larger AgNSs with a broader size distribution were obtained in the absence of starch (C) with [$AgNO_3$] of 0.14 mM. When a 117 μL of 30% H_2O_2 was injected into a 40 mL colloid of the non-stabilized AgNSs (C), only the disintegration of metallic AgNSs was attained without any shape transformation (D). The shape transformation of starch-stabilized AgNSs can always be triggered by an addition of H_2O_2 as shown in Fig. 1 (main text). The observed phenomena indicate a crucial role of starch as a stabilizer assisting the shape transformation process from AgNSs to AgNPrs.

Fig. S6 Experimental verification on the formation of Ag_2O in 2% (w/v) soluble starch (A) and DI water (B) at pH 10.

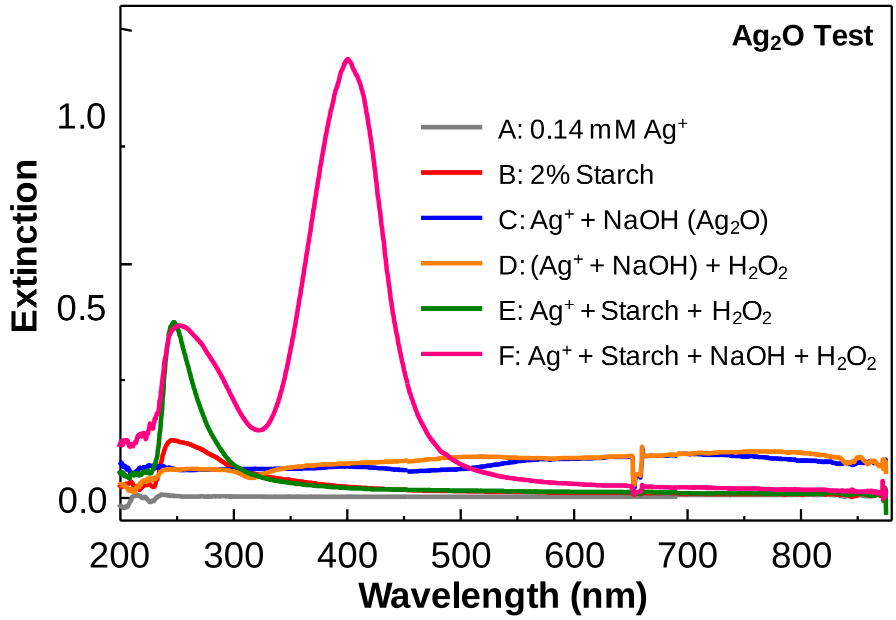

Fig. S7 UV-visible spectra of Ag^+ (A), 2% (w/v) soluble starch (B), Ag_2O in DI water (C), Ag_2O + H_2O_2 in DI water (D), a mixture of Ag^+ and H_2O_2 in 2% (w/v) soluble starch solution at pH 7 (E), and yellow colloid from the reaction of Ag^+ and H_2O_2 in 2% (w/v) soluble starch at pH 10 (F).

In order to investigate whether Ag_2O existed in the shape transformation process or not, two type of reaction media i.e. 2% (w/v) soluble starch and DI water with pH 10 were prepared before the injection of Ag^+ having final concentration of 0.14 mM. The results are shown in Fig. S6. Cloudy solution was observed only when DI water was used as the reaction medium. Although the solution is moderate alkaline of pH 10, starch can prohibit the formation of Ag_2O through the binding of Ag^+ with ether oxygen and hydroxyl groups of the starch molecules (J. He, T. Kunitake, and A. Nakao, *Chem. Mater.*, 2003, 15, 4401–4406.) as a clear solution was observed after 60 s incubation. These phenomena suggest that Ag_2O does not exist in the shape transformation process as the oxidatively dissolved Ag^+ ions are rapidly complex with starch. The complex is strong enough to inhibit the formation of Ag_2O. When H_2O_2 was added to the solution of soluble starch stabilized Ag^+, the orange-yellow color developed immediately. The plasmon extinction spectrum of that yellow solution is shown in Fig. S7. The characteristic DPR centered at 400 nm with the absorption at 220–320 nm of the interband transition suggests the formation of spherical silver nanoparticles. However, in the system without starch stabilizer, no DPR is observed in UV-Vis spectra of Ag_2O solution as well as its product after an addition of H_2O_2. A large amount of gas bubbles observed during the reaction was due to the alkaline-catalyzed decomposition of H_2O_2 (F. R. Duke and T. W. Hass, *J. Phys. Chem.*, 1961, 65, 2, 304–306.). These observations also suggest that H_2O_2 is the sole reducing agent in the shape transformation process since the reduction by starch under the employed conditions does not occur.

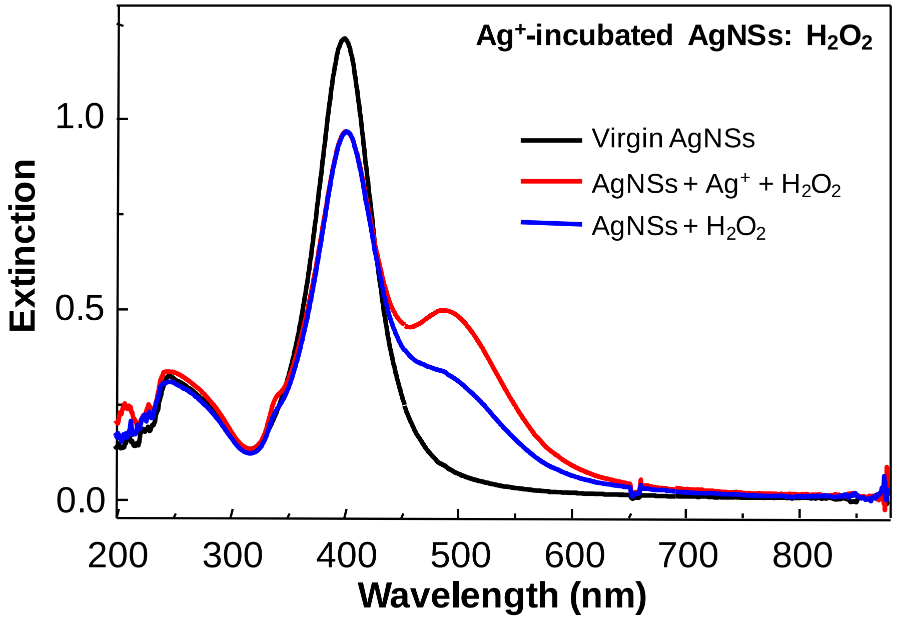

Fig. S8 Plasmon extinction spectra of AgNSs, AgNSs + H_2O_2, and Ag^+-spiked AgNSs + H_2O_2. The systems with and without added Ag^+ show the same degree of etching of the original AgNSs. A greater number of AgNPrs was generating from the system with added Ag^+. The experimental parameters: AgNSs (3.52 mM, 38 mL); $AgNO_3$ (9.27 mM, 2 mL) or DI Water (2 mL); H_2O_2 (30% (w/w), 117 μL).

To corroborate the idea that H_2O_2 plays the dual functions as the oxidative etchant and reducing agent, a shape transformation with an addition of extra $AgNO_3$ was performed. When 117 μL of 30% H_2O_2 was added to the Ag^+-spiked AgNSs, a greater extinction of IPDPR at 500 nm was achieved (i.e., compared to the operation on AgNSs without an additional Ag^+). The greater IPDPR at 500 nm due to a greater concentration of AgNPrs is attributed to the reduction of additional Ag^+ by H_2O_2. The added Ag^+ ions increase the concentration of metal ions necessary for the formation of silver atoms required for the development of AgNPrs. AgNSs were etched by H_2O_2 as observed by the decrement of the DPR extinction at 400 nm. Interestingly, extents of the AgNSs etching of the two colloids are equivalent since the DPR extinctions at 400 nm are decreased by the same magnitude. This simple experiment clearly demonstrates the oxidation and reduction capabilities of H_2O_2 in the shape transformation process. H_2O_2 oxidatively etches AgNSs while it reduces Ag^+ to Ag atoms. The formation of AgNPrs from the dissolved Ag^+ is evident as the extinction at 400 nm decreases with a concomitant development of the extinction at 500 nm after an addition H_2O_2.

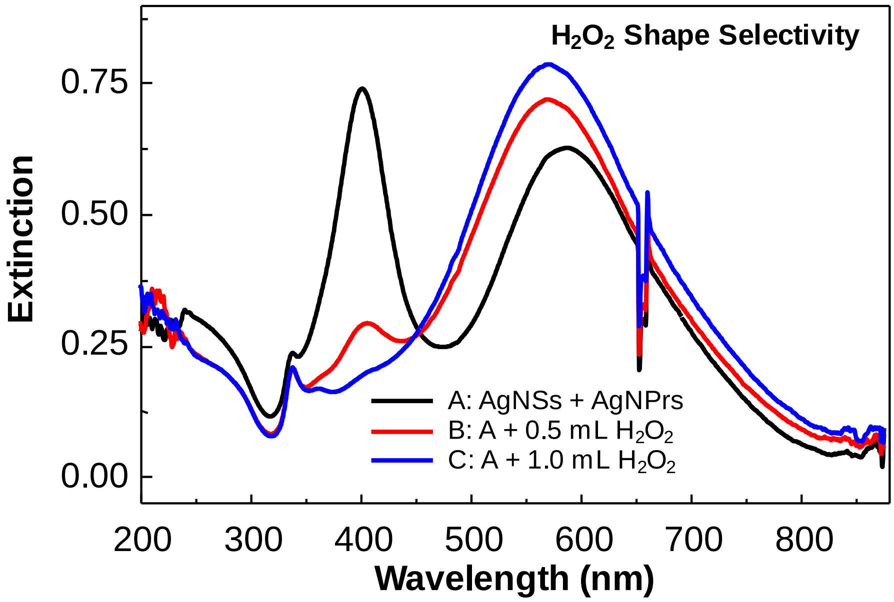

Fig. S9 Plasmon extinction spectra show a selective etching of H_2O_2 toward AgNSs. AgNSs were completely dissolved when a larger volume of H_2O_2 was employed. An evidence of sculpturing of AgNPrs is noticed by the blueshift of the IPDPR from 588 to 570 nm. These observed phenomena are different from those shown in Kawazumi's paper as we employed a relatively low concentration of H_2O_2. As a result, a complete dissolution of both AgNSs and AgNPrs was not observed. In the contrary, a formation of a greater concentration of AgNPrs was observed as a greater volume of H_2O_2 was employed. The experimental conditions: AgNSs (3.71 mM, 100 mL), AgNPrs (3.71 mM, 100 mL), H_2O_2 (0.5-1 mL).

It has been shown by Kawazumi's paper (M. Tsuji, S. Gomi, Y. Maeda, M. Matsunaga, S. Hikino, K. Uto, T. Tsuji and H. Kawazumi, *Langmuir*, 2012, 28, 8845–8861) that nanoplates are more tolerant to the oxidative etching of H_2O_2 than nanospheres. In our case, when H_2O_2 was injected to the colloidal mixture (1:1 (v/v)) of AgNSs (DPR = 400 nm) and AgNPrs (IPDPR = 588 nm), H_2O_2 preferentially destroyed AgNSs while promoted the growth of AgNPrs. DPR intensity of AgNSs is reduced indicating the oxidative dissolution of AgNSs. An increment in the IPDPR intensity of AgNPrs suggests an increase AgNPrs population. However, the original AgNPrs were also etched as indicated by the blueshift of IPDPR from 588 nm to 570 nm.

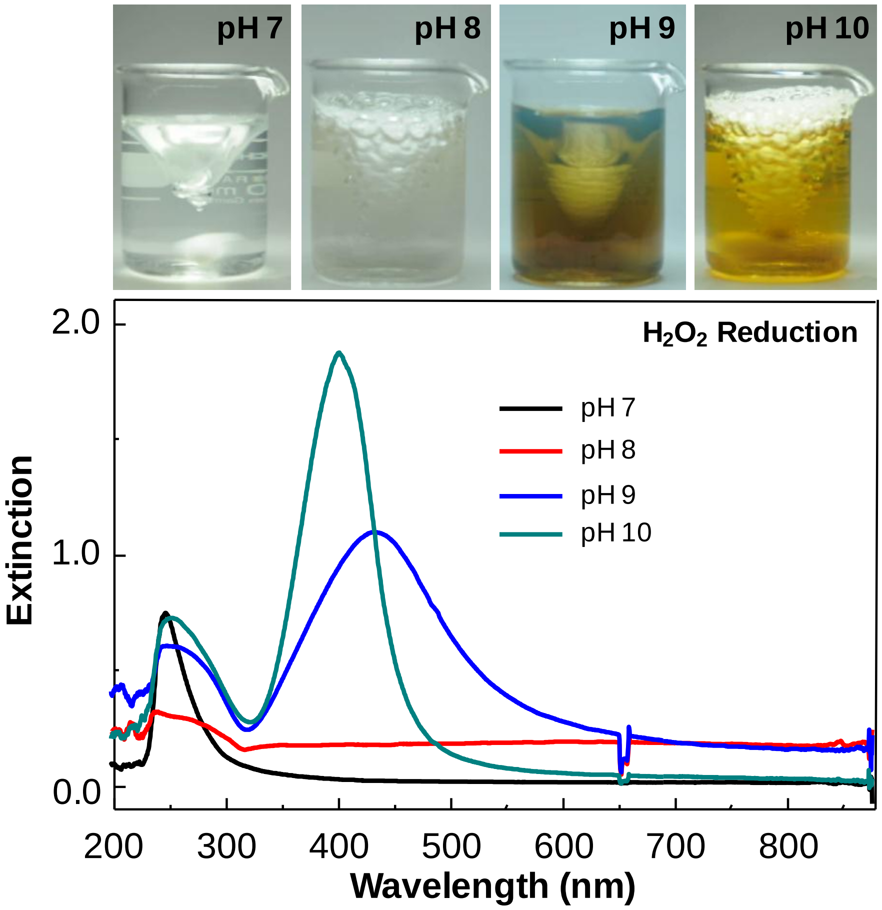

Fig. S10 UV-visible spectra of solutions when 0.14 mM Ag^+ in 2% (w/v) soluble starch were reduced with H_2O_2 at various pH. The experimental procedure is the same as indicated in Fig. S6 except for the volume of 1 M NaOH injected to obtain the specified pH. The reduction of Ag^+ did not occur at pH 7.

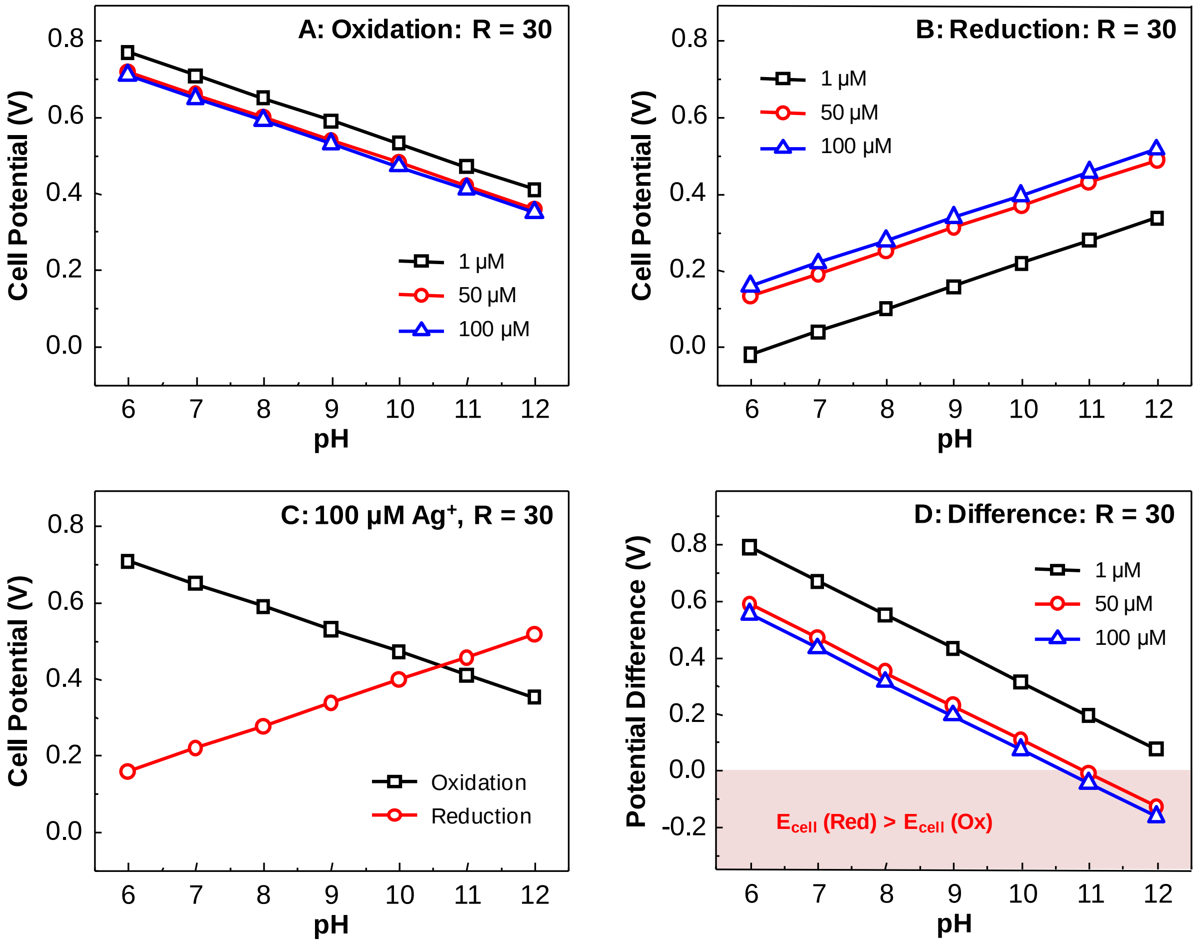

Fig. S11 Plots of the oxidation cell potential (A), the reduction cell potential (B), comparison of the oxidation and reduction cell potentials (C), and the difference (oxidation – reduction) potential (D) as a function of pH. The cell potentials are calculated by Nernst equation with the concentrations according to those employed in the shape transformation process. The influence of Ag$^+$ concentrations (i.e., 1, 50, and 100 μM) are compared in (A) and (B) for the oxidation and reduction cell potentials, respectively. The reduction is dominant at high pH and/or high Ag$^+$ concentration. The molar ratio R of H_2O_2:Ag$^+$ is 30. The temperature is set at 301.15 K. The pressure of evolved oxygen gas is assumed the ambient pressure.

The electrochemical cell potentials of oxidative etching of AgNSs and reduction of Ag^+ with H_2O_2 can be described with the following equations:

Oxidation: $2Ag + H_2O_2 = 2Ag^+ + 2HO^-$ $\quad E^0_{cell}\left(Ox\right) = 0.068\,V$

Reduction: $H_2O_2 + 2Ag^+ + 2HO^- = 2Ag + 2H_2O + O_2$ $\quad E^0_{cell}\left(Red\right) = 0.947\,V$

The oxidation and reduction cell potentials are dependent on pH as suggested by the Nernst equations. The cell potentials at various concentrations of Ag^+ and OH^- can be expressed by the following equations:

$$E_{cell}\left(Ox\right) = 0.068 - \frac{RT}{nF}\ln\frac{[Ag^+]^2[OH^-]^2}{[H_2O_2]}$$

$$E_{cell}\left(Red\right) = 0.947 - \frac{RT}{nF}\ln\frac{p(O_2)}{[Ag^+]^2[OH^-]^2[H_2O_2]} = 0.947 - \frac{RT}{nF}\ln\frac{1}{[Ag^+]^2[OH^-]^2[H_2O_2]}$$

For simplicity, the pressure of oxygen gas evolved during the reaction is approximately set equal to 1 atm. Based on the above expressions, the difference between the oxidation and oxidation cell potentials can be simplified as:

$$E_{cell}\left(Diff\right) = E_{cell}\left(Ox\right) - E_{cell}\left(Red\right) = -0.879 - 4\frac{RT}{nF}\ln[Ag^+][OH^-]$$

The oxidation cell potential is a decreasing function, while the reduction cell potential is an increasing function with respect to the concentration of OH^- (Fig. S11 A and B). The alkaline medium enhances the reducing capability of H_2O_2 while its oxidizing activity is partially suppressed. The reduction cell potential is significantly increased in comparison to the oxidation cell potential when Ag^+ concentration or pH is increased. The oxidation and reduction cell potentials possess the positive values in the range of pH from 7–12 suggesting H_2O_2 is capable of both oxidation and reduction. The potential gap between oxidation and reduction reaction is narrowed down when pH of the solution is increased. These suggest that both reactions may competitively occur in alkaline medium. The result of this concerted oxidation/reduction is the shape transformation of AgNSs to AgNPrs. However, this conclusion is valid only at a relatively low concentration of H_2O_2. At a high concentration of H_2O_2, more complicated reactions of H_2O_2 and Ag metal may occur such as an autocatalytic decomposition of H_2O_2 on the surface of silver metal.

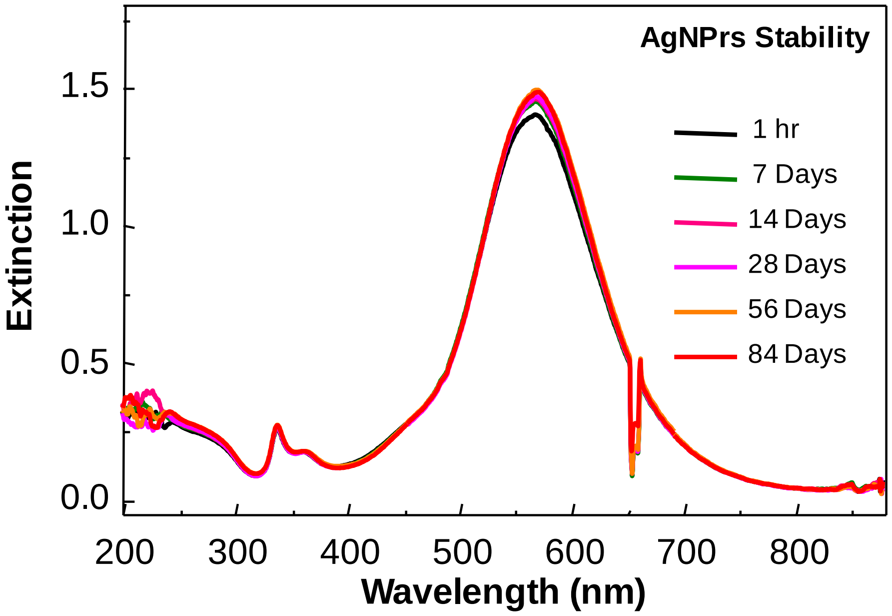

Fig. S12 Plasmon extinction spectra reveal the stability of AgNPrs under a prolong storage. The AgNPrs colloid was synthesized at the concentration of 3.71 mM. The colloid was stored under the ambient conditions without additional purification. For quantitative comparison, the measured colloids were diluted to 92.7 µM by deionized water before each measurement. An insignificant spectral change after a 3-month storage suggests that AgNPrs are very stable under the synthetic environment. An absent of the absorption at 250-270 nm indicates that H_2O_2 is completely consumed by the shape conversion process (see also Fig. S14 for UV-Vis spectra of various reagents).

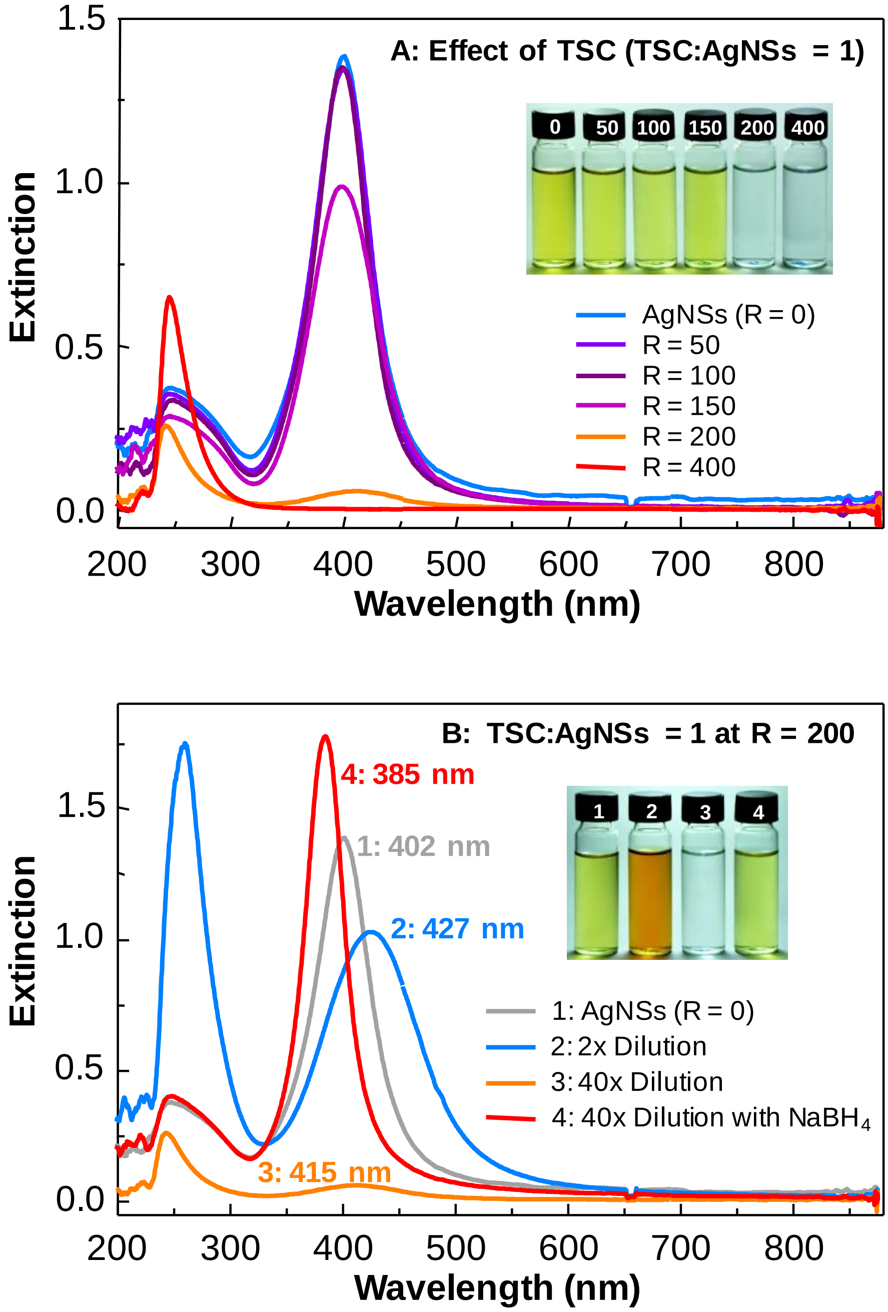

Fig. S13 The effect of trisodium citrate (TSC) on the AgNPrs development at various molar ratio of H_2O_2:AgNSs (R) (A). Comparison of the extinction spectra of the AgNSs (1), AgNSs+TSC+H_2O_2 at R = 200 with various dilution factors (2 and 3), and the suspension 3 after an addition of $NaBH_4$ (4) is also shown (B). The experimental parameters were the same as indicated in the experimental section except that TSC was added to in AgNSs with the molar ratio of TSC:AgNSs = 1 before the injection of H_2O_2 solution.

The observed phenomena in Fig. S13A suggest that TSC inhibit the shape transformation process induced by H_2O_2. When a greater mole ratio R was employed, dissolution of AgNSs without a formation of AgNPrs was achieved. A completed dissolution was obtained with the mole ratio R greater than 200. The dissolved Ag^+ is expected to form a stable complex with citrate. The complex could withstand the weak reduction potential of H_2O_2. However, when $NaBH_4$ was added into the oxidatively dissolved Ag^+, small AgNSs with DPR of 385 was obtained (Figs. S13B).

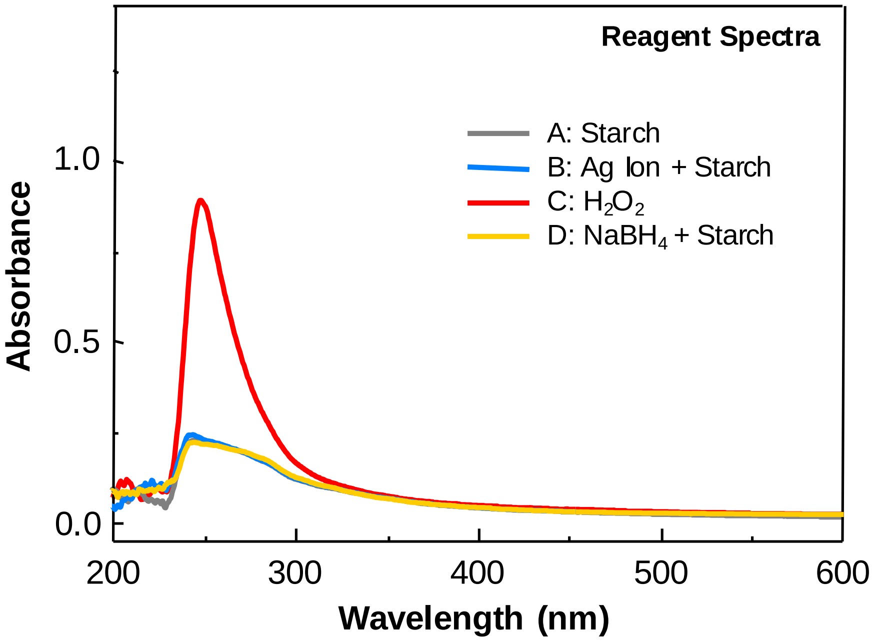

Fig. S14 UV-visible spectra of reagents employed in the H_2O_2-induced shape transformation of AgNSs to AgNPrs including starch solution, Ag^+ in starch solution, H_2O_2 solution, and $NaBH_4$ in starch solution.

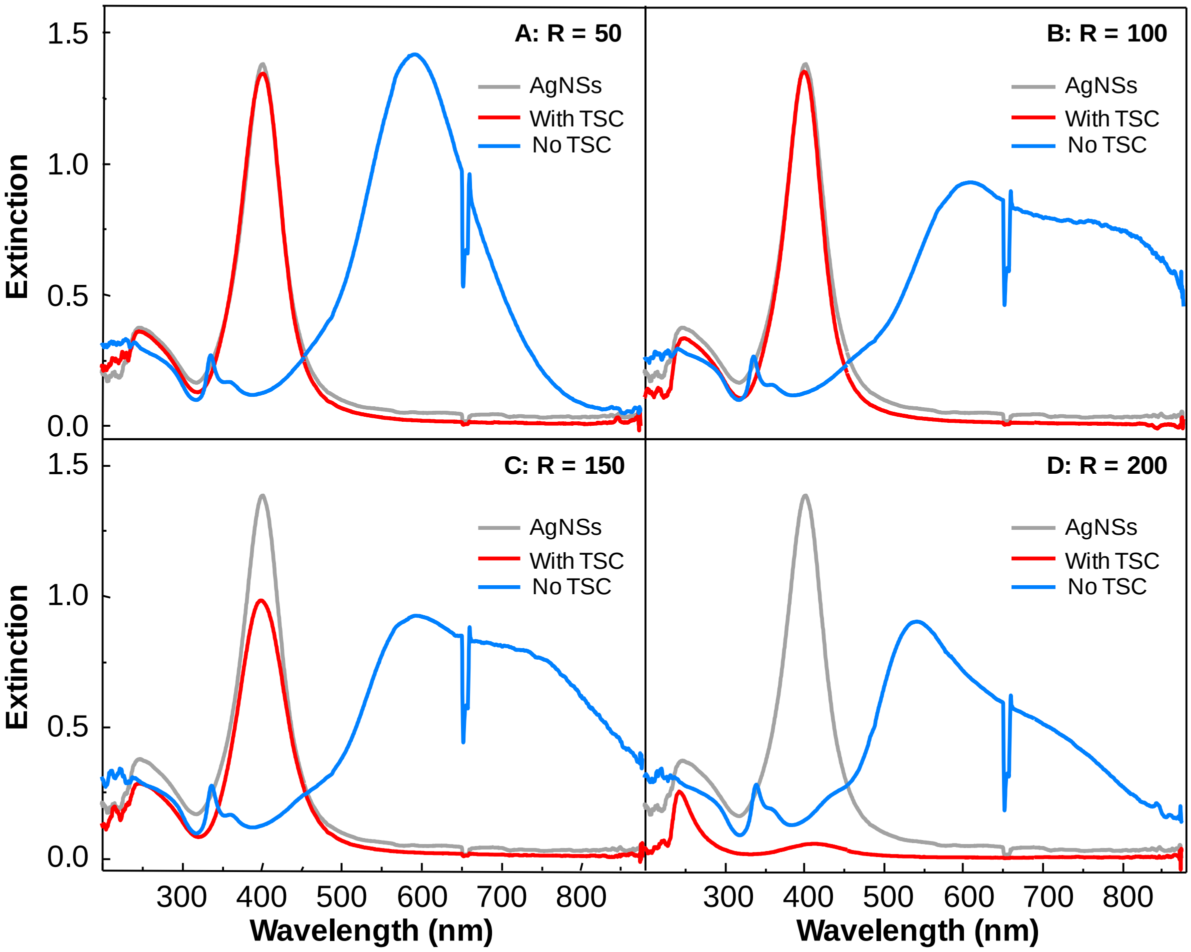

Fig. S15 The effect of trisodium citrate (TSC) on the AgNPrs development at various molar ratio of H_2O_2:AgNSs (R). Extinction spectra of AgNSs, AgNSs+H_2O_2, and AgNSs+TSC+H_2O_2 are compared in each panel.

The shape transformation induced by H_2O_2 did not occur when TSC is present in the system. The oxidatively dissolved Ag^+ is expected to form a stable complex with TSC. The Ag-TSC complex is stable and cannot be reduced by the weak reducing capability of H_2O_2. An extensive dissolution was observed when a greater concentration of H_2O_2 was employed. A shape transformation from AgNSs to AgNPrs was achieved under an identical experimental condition without TSC.

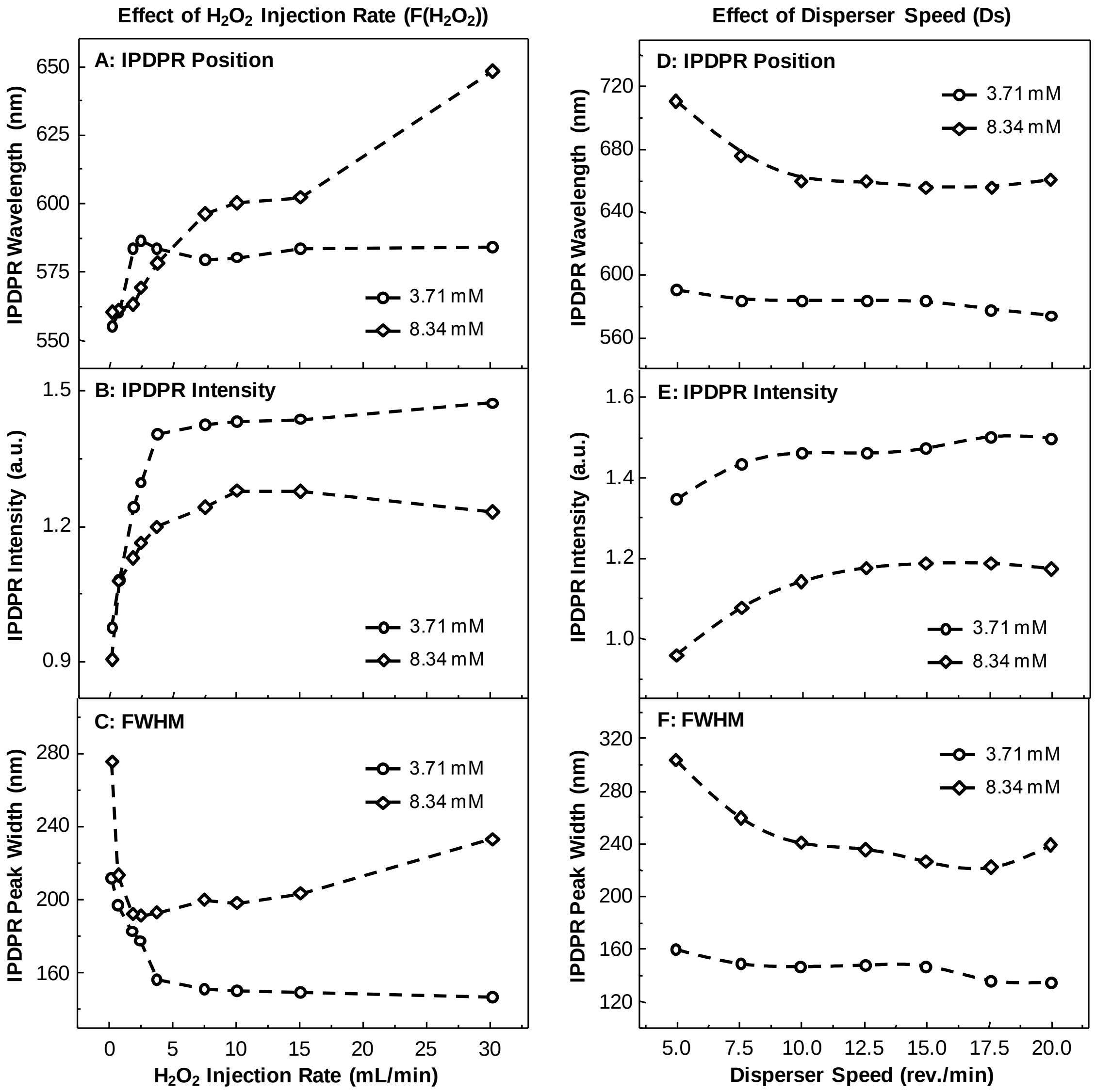

Fig. S16 The effect of initial AgNSs concentration, H_2O_2 injection rates (F(H_2O_2)) (A–C) and disperser speed (Ds) (D–F) on IPDPR peak characteristics of AgNPrs: peak position (A and D), intensity (B and E), and full width at half maximum (FWHM) (C and F). Initial AgNSs concentrations were 3.71 mM and 8.34 mM. The experimental parameters are the same as indicated in Fig. 4 (main text).

Table S2 The optimal experimental parameters for synthesizing AgNPrs corresponding to the extinction spectra in Fig. 5 (main text)**.** AgNSs colloid of different concentration requires different concentration of H_2O_2 to optimally tune the LSPR wavelength across the visible region with a complete conversion of AgNSs to AgNPrs. A greater mole ratio R is required for a colloid with a greater concentration of AgNSs. A greater redshift of the IPDPR was obtained when colloid with a greater concentration of AgNSs was employed.

Exp No.	AgNPs Concentration	AgNS:H_2O_2 (mole ratio)	H_2O_2 Flow Rates (mL/min)	Out-of-Plane Quadrupole Plasmon Resonance Wavelength (nm)	In-Plane Dipole Plasmon Resonance Wavelength (nm)
1	100 ppm (0.927 mM)	1:20	25.22	346	461
2		1:5		342	487
3	200 ppm (1.854 mM)	1:20	10.09	341	500
4	300 ppm (2.781 mM)	1:20	5.045	339	535
5	400 ppm (3.708 mM)	1:30	13.45	338	557
6	500 ppm (4.635 mM)	1:30	18.92	337	592
7	600 ppm (5.562 mM)	1:40	22.70	336	617
8	700 ppm (6.489 mM)	1:40	35.31	336	637
9	800 ppm (7.416 mM)	1:40	40.36	336	652
10	900 ppm (8.344 mM)	1:40	56.75	336	670
11	1000 ppm (9.270 mM)	1:50	68.79	336	700
12	1100 ppm (10.198 mM)	1:70	69.36	335	759
13	1200 ppm (11.125 mM)	1:90	70.66	335	830

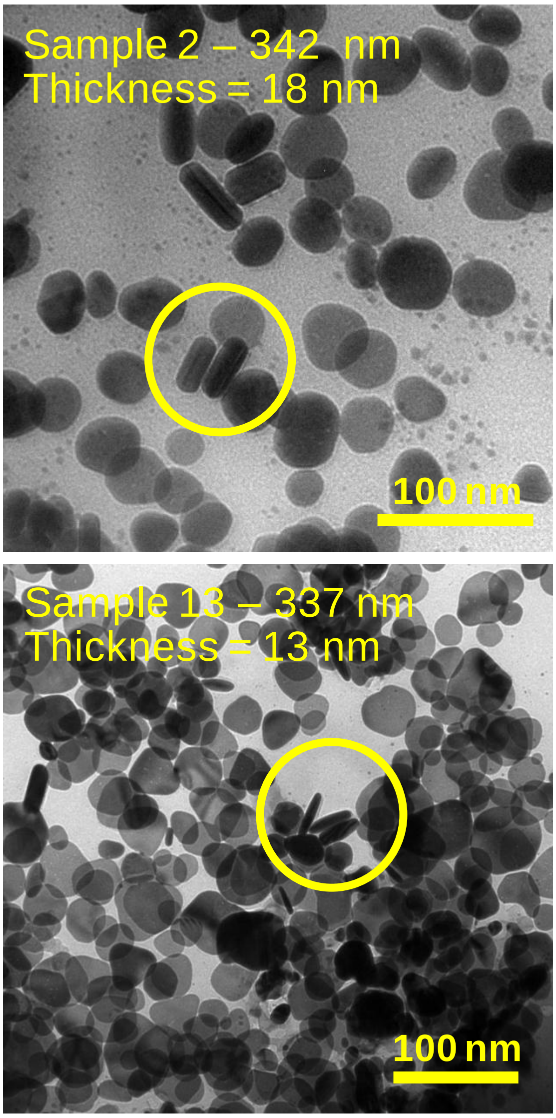

Fig. S17 TEM micrographs of AgNPrs aligned edge-on to the electron beam. The sample numbers is corresponding to the extinction spectra of Fig. 5 (main text). The out-of-plane quadrupole plasmon resonance (OPQPR) wavelengths are indicated.